



Effects of chemical and autoclave sterilization treatments on medical personal protective equipment made of nonwoven polypropylene fibers for recycling

Pixiang Wang¹ · William D. Cutts¹ · Haibin Ning² · Selvam Pillay² · Shaoyang Liu¹

Received: 6 April 2022 / Accepted: 28 July 2022 / Published online: 2 August 2022
© The Polymer Society, Taipei 2022

Abstract

Medical personal protective equipment (PPE) made from nonwoven thermoplastic fibers has been intensively used, resulting in a large amount of biohazardous waste. Sterilization is indispensable before recycling medical waste. The aim of this work is to evaluate the effects of the decontamination treatments and help properly recycle the PPE materials. The study investigated the effects of three disinfection treatments (NaClO, H₂O₂, and autoclave) on chemical composition, molecular weight, thermal properties, crystallinity, crystallization kinetics, and mechanical tension of three types of PPE (Gown #1, Gown #2, and Wrap) made of isotactic polypropylene fibers. The chemical compositions of the materials were not evidently affected by any of the treatments. However, the M_w of the polymers decreased about 2–7% after the treatments, although the changes were not statistically significant. The treatments barely affected the melting and crystallization temperatures and the maximum force at break, but they tended to elevate the thermal degradation temperatures. Although the treatments did not notably influence the crystallinities, crystallization rates and crystal growths were altered based on the Avrami model regression. Since the detected changes would not significantly affect polymer processing, the treated materials were suitable for recycling. Meanwhile, evident differences in the three types of raw materials were recorded. Their initial properties fluctuated notably, and they often behaved differently during the treatments, which could affect recycling operation. Recyclers should test and sort the raw materials to assure product quality. The results in this study provide fundamental data for recycling medical PPE to reduce its environmental footprint.

Keywords PPE · Recycle · Sterilization · M_w · Crystallization kinetics · Avrami model

Introduction

Single-use personal protective equipment (PPE), such as gowns, wraps, face shields, gloves, masks, shoe coverings, head coverings, etc., has been widely applied for hygiene protection and safety for doctors, nurses, and patients because of their cost-effectiveness, lightweight and good protection [1]. Nonwoven thermoplastic fibers, of which polypropylene (PP) and polyethylene terephthalate (PET)

comprise the majority, are popular materials to manufacture various types of PPE. They are broadly used to make gowns, wraps and face masks. The PPE are made of two- or three-layered laminates that are thermally bonded, which provide efficient protection from human fluids, pathogenic microorganisms, airborne microparticles, chemical spills, etc. [2].

The extensive use of disposable PPE generates a large amount of waste. The associated environmental influence has attracted more and more attention in recent years. A public health emergence, such as the COVID-19 pandemic, could further worsen the situation and dramatically increase the medical waste all over the world due to the significantly elevated consumption of PPE. It was estimated that the COVID-19 pandemic would result in six times more PPE waste than normal, which is an enormous amount of materials that will mainly either go into landfills or be incinerated [3, 4]. Both of the disposal methods are harmful to the

✉ Shaoyang Liu
lius@troy.edu

¹ Center for Materials and Manufacturing Sciences,
Department of Chemistry and Physics, Troy University,
Troy, AL 36082, USA

² Department of Materials Science & Engineering, University
of Alabama at Birmingham, Birmingham, AL 35294, USA

environment and an opportunity to recycle and repurpose the materials is lost [5, 6].

PPE recycling is a meaningful way to deal with its rapid growth. Due to the contamination of infectious and pathological microorganisms, used PPE is considered as a biohazard and needs to be sterilized before disposal or recycle by EPA regulation. There are several sterilization methods available, including incineration, autoclaving, chemical treatments, UV treatment, plasma disinfection, and microwave treatment [7]. Incineration is the process of destroying waste by burning it at elevated temperatures in furnaces. It is a common PPE disposal method, which greatly reduces the waste amount. However, it completely destroys the materials and has disadvantages such as high cost, smoke generation, and pollution risks. In particular, incineration of medical PPE waste produces more furans and dioxins than municipal waste [7]. Autoclave sterilizes PPE by using steam, heat, and pressure during a specific time frame, which is usually at 121 °C for about 15 to 35 min depending on the size of the load and the contents [8]. Chemical treatments often employ highly reactive reagents, including hydrogen peroxide or sodium hypochlorite. Solid PPE wastes need to be shredded before chemical treatments for adequate disinfection, and unexpected chemical reactions might occur when pharmaceuticals present [7]. UV irradiation is a newly studied method to decontaminate PPE for repeated use [9], but the poor penetration ability of UV lights raises a concern of achieving full decontamination, especially for solid PPE [10, 11]. Microwaves can achieve full sterilization in just a couple of minutes, but the PPE must be properly shredded and moisture-corrected before the treatment [12].

Among the available decontamination techniques, autoclave and chemical treatments are more convenient and robust to achieve complete sterilization for recycling. However, autoclave involves high temperature and pressure and thus may degrade the PPE polymer materials. Grinshpun et al. had evaluated common PPE masks with respect to the changes in their performance and integrity resulting from autoclave sterilization [8]. The results showed that the initial collection efficiency and the filter breathability of masks might be compromised by autoclave and physical damages were also observed. Active reagents used in chemical treatments could also degrade the polymers, affect the chemical structures of the PPE materials, and react with additives in the polymers [13, 14]. Thus, there is a pressing need to evaluate the PPE materials after the disinfection treatments to understand their changes for proper recycling.

In the present study, an attempt had been made to characterize the effects of sterilization treatments on medical PPE materials. Since gown has a big size and is the second most commonly used PPE item [15], and wrap has a large size, they account for a large portion of the PPE waste in healthcare setting and would be most economically feasible

to recycle. Therefore, two types of gowns and one type of wrap made of nonwoven PP fibers were investigated in this work. Chemical compositions, molecular weights, thermal properties, crystallization kinetics, and mechanical tensions of the three types of PPE materials were monitored before and after autoclave, as well as NaClO and H₂O₂ treatments. The results provide fundamental information of PPE materials subject to disinfection treatments and will benefit recycling and repurposing single-use medical PPE waste.

Materials and methods

Materials

Three types of PPE (Gown #1, Gown #2, and Wrap) were provided by the University of Alabama at Birmingham Hospital. Non-biohazardous disposed PPE was used to mimic actual PPE wastes. They were the same PPE the hospital used except for not being exposed to any biohazards in medical operations. The Gown #1 and Wrap were made in Myanmar and distributed in the US by Medline Industries, Inc. (Northfield, IL, USA). The Gown #2 was manufactured in China. The thicknesses of Gown #1, Gown #2, and Wrap were 0.20 ± 0.01 mm, 0.10 ± 0.01 mm and 0.26 ± 0.02 mm, respectively. They are all made of nonwoven PP fibers. All chemicals used in this study were analytical grade and supplied by Fisher Scientific (Waltham, MA, USA).

Sterilization of PPE

The PPE materials were cut into about 2 cm × 4 cm pieces before treatments. The autoclave treatment was carried out with a “waste” program of a steam sterilization autoclave (Steris AMSCO LS250) [16]. The samples were sterilized at 121 °C for 35 min under a pressure of 0.1 MPa (15 psi). Chemical treatments were performed in either 0.6% NaClO or 8% H₂O₂ solution following the CDC guidelines [17]. Briefly, 0.30 g of the PPE sample was added to 100 mL NaClO or H₂O₂ solution in a 250 mL Erlenmeyer flask. The mixture was shaken on a multi-platform mixer (Model: 1387700, Fisher Scientific, Waltham, MA, USA) at 250 rpm under room temperatures for 60 min to allow the PPE to sufficiently interact with the sterilization solution. After the treatments, the PPE sample was separated from the solution by filtration with Buchner funnel and washed with deionized water five times. Finally, the PPE was air-dried in a fume hood overnight before tests. Since the main goal of this work is to investigate the effects on the materials, not the decontamination efficiency, only well-established sterilization methods were selected, and complete decontamination was expected after the treatments.

PPE material characterization

Chemical compositions of the PPE before and after the treatments were analyzed with IR spectrometry. An FT-IR spectrophotometer with ATR sampling accessory (Spectrum Two, Perkin-Elmer, Waltham, MA, USA) was employed to record the spectrum in the wavenumber range of 450 to 4000 cm^{-1} with a resolution of 4 cm^{-1} . An average of 32 scans was recorded to reduce the noise. Spectrum v10.5.3 (Perkin-Elmer, Waltham, MA) was used to analyze the data.

A Raman spectrometer equipped with a 785-nm laser (MacroRAM, Horiba Scientific, Piscataway, NJ, USA) was employed to collect the spectrum in a Raman shift range of 100–3400 cm^{-1} . The average of 5 measurements was recorded to reduce noise. LabSpec 6 (Horiba Scientific, Piscataway, NJ, USA) was used to acquire and process the data. The spectra were smoothed by the DeNoise function, the baselines were corrected by polynomial curve fitting, and the peaks were normalized based on the maximum peak in the displayed range. The identification was carried out with KnowItAll Raman spectral library (Horiba Edition, Wiley Science Solutions).

Molecular weights and distributions of the PPE materials were analyzed with a gel permeation chromatograph with an infrared detector (GPC-IR, Polymer Char, Valencia, Spain). The GPC separation was carried out by three PLgel Olexis 300 $\text{mm} \times 7.5 \text{ mm}$ columns (Agilent, CA, USA). The operation temperature was 160 $^{\circ}\text{C}$, the mobile phase was 1,2,4-trichlorobenzene (TCB), the flow rate was 1 mL/min , and the injection volume was 200 μL . The samples were dissolved in TCB at 160 $^{\circ}\text{C}$. The sample concentrations were about 1 mg/mL [18]. The GPC tests were carried out in triplicates.

Thermogravimetric analyses (TGA) were performed using a TGA-550 (TA Instruments, DE, USA) with platinum-HT sample pans. About 10 to 15 mg of PPE samples were used in each run. The measurements were carried out under a nitrogen environment with gas flows of 60 mL/min for sample purge and 40 mL/min for balance purge. The temperature raised from room temperature to 600 $^{\circ}\text{C}$ at a heating rate of 20 $^{\circ}\text{C}/\text{min}$. Each PPE sample was measured three times [19]. For evaluation, TGA curves were normalized based on starting weight. Data analysis was achieved by using TRIOS Software (TA Instruments, DE, USA). DTG curves (the first derivation of thermal gravimetry) were used to determine the mass loss percentage ($\%/\text{C}$).

Differential scanning calorimetry (DSC) measurements were carried out with a DSC-250 using Tzero Pans (TA Instruments, DE, USA). About 10 to 15 mg of PPE samples were used in each run. The PPE samples were first heated from 40 $^{\circ}\text{C}$ to 200 $^{\circ}\text{C}$ at a rate of 20 $^{\circ}\text{C}/\text{min}$ to remove their thermal history. Then, the samples were cooled to 40 $^{\circ}\text{C}$ at a rate of 10 $^{\circ}\text{C}/\text{min}$ to trace the crystallization process.

They were again heated to 200 $^{\circ}\text{C}$ at the rate of 20 $^{\circ}\text{C}/\text{min}$ to record their melting behaviors. For determining crystallization activation energy, the cooling rates of 5, 10 and 15 $^{\circ}\text{C}/\text{min}$ were employed. Each sample was measured in triplicates. The data analysis was performed with TRIOS software (TA Instruments, DE, USA). The crystallinity was calculated based on the heat of fusion of 100% crystalline polymer (207 J/g for polypropylene) [20, 21]. Since some samples had high ash contents and the ash was not a part of the polymer, the crystallinity was corrected by the following equation:

$$\text{Crystallinity}(\%) = \frac{\text{Melting enthalpy}}{207 \times (1 - \text{ash content}(\%))}$$

For mechanical property analysis, the PPE specimens of 1.0 cm wide were tested in tension mode with a universal mechanical test system (INSTRON 5966, Instron, MA, USA). The testing speed was 10 mm/min , and each PPE sample was measured five times.

Statistical analysis

All statistical analyses were carried out with Tukey's HSD test and conducted using SAS software (SAS Institute Inc, Cary, NC). Results with p-values below the conventional 5% threshold were regarded as significant.

Results and discussion

Chemical composition of the PPE materials and changes after the sterilization treatments

Single-use gowns and wraps are typically constructed of nonwoven materials alone or in combination with materials that offer increased protection from liquid penetration. The basic raw materials commonly used are various forms of synthetic fibers, such as PP, PET, polyester, polyethylene, etc. These fibers can be produced using a variety of nonwoven fiber-bonding technologies (thermal, chemical, or mechanical) to provide integrity and strength [22].

Each of the three types of PPE studied in this work was made of only one type of nonwoven PP fibers, one of the most common materials for the purpose. The chemical nature was confirmed with IR analysis. As shown in Fig. 1, the same dominant IR absorption peaks were observed for all three types of materials before the treatments. The absorption bands in 2850–2960 cm^{-1} are corresponding to the symmetric and asymmetric stretching of CH_3 and CH_2 groups, while the symmetric and asymmetric bending absorptions of CH_3 group are observed at around 1390 and 1470 cm^{-1} , respectively [23]. The characteristic bands are

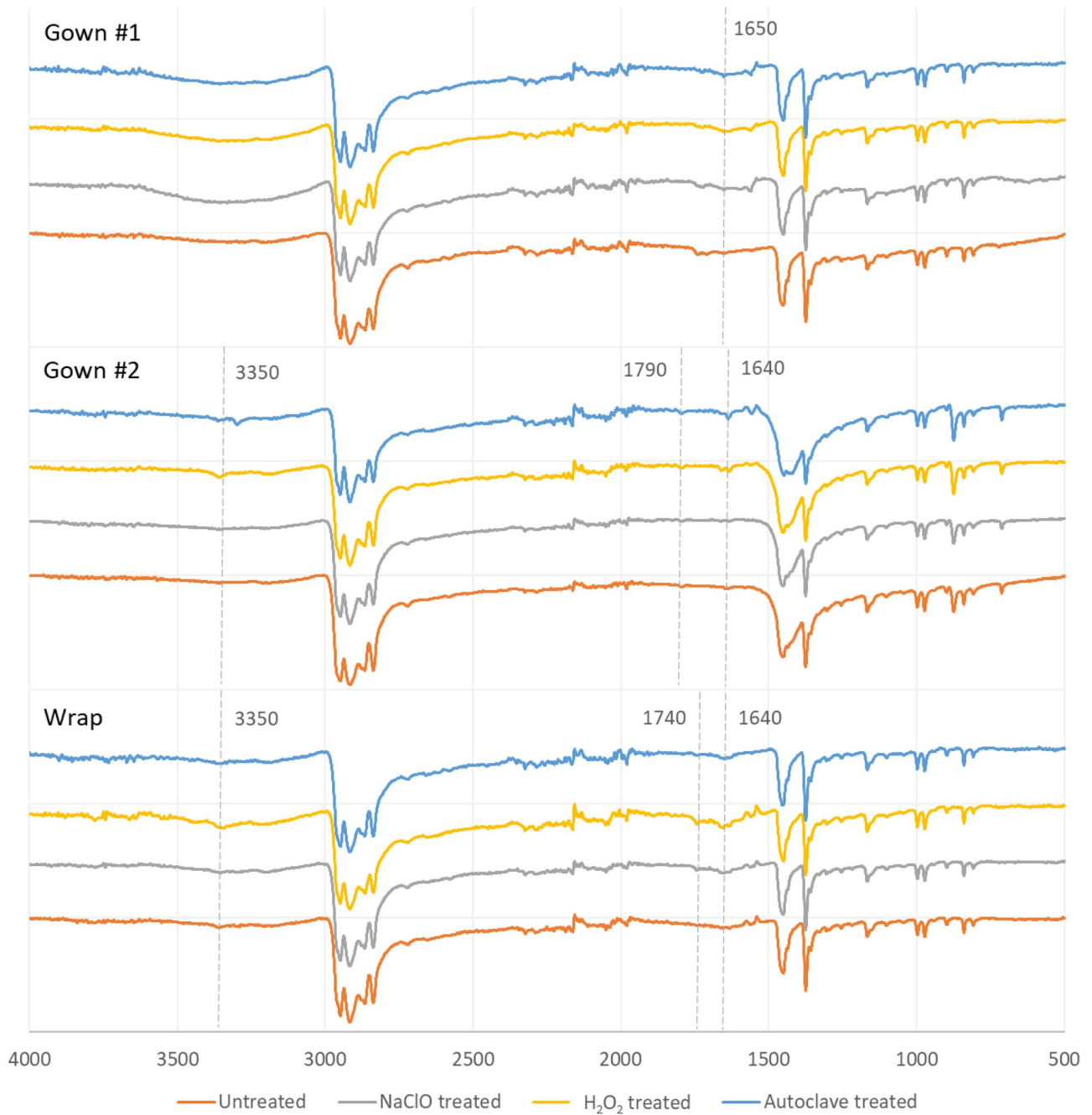


Fig. 1 FT-IR spectra of the three types of PPE materials with or without treatments

identical to those of isotactic polypropylene [24, 25], which confirmed that all three types of PPE were made of isotactic polypropylene fibers.

Since strong disinfection treatments were employed to ensure complete sterilization of the medical PPE, there was a concern if the treatments would notably change the chemical composition of the materials. The IR spectra of the treated PPE are also illustrated in Fig. 1 to evaluate the effects of the treatments. No evident change was

observed on all the dominant bands, suggesting that the treatments did not significantly change the major composition of the materials. However, some minor differences in the IR spectra were found after some treatments. For example, small peaks at around 1650, 1750, and 3350 cm^{-1} appeared after the H_2O_2 and autoclave treatments of Gown #2 and the H_2O_2 treatment of the Wrap. The bands at around 1650 and 1750 cm^{-1} are corresponding to the C=C and C=O stretching, respectively, while

the absorptions at around 3350 cm^{-1} could be assigned to stretching of OH groups. Minor peaks at around 1650 and 1750 cm^{-1} were also found after the autoclave and NaClO treatments of the Wrap. In addition, subtle peaks at around 1650 cm^{-1} slightly strengthened after the H_2O_2 , NaClO, and autoclave treatments of Gown #1. These changes suggested that some treatments might slightly oxidize the polymer and introduced a small number of double bonds to the polymers. However, given the low absorptions of the peaks and high molar absorptivities of the corresponding chemical bonds, the changes in chemical composition caused by the treatments were essentially negligible, and the treated PPE materials were still dominantly composed of PP.

Figure 2 illustrates the Raman spectra of the untreated and treated samples for all three types of materials. No evident change was observed when comparing the untreated and treated samples of the same type of material. The results confirmed that the disinfection treatments did not notably alter the chemical compositions of the materials. Moreover, when comparing the spectra to that of pure PP, insights into the additives in the three types of materials were obtained. For example, the Raman spectra of Gown #2 samples showed three additional peaks at 285 , 715 , and 1084 cm^{-1} , respectively (Fig. 2, middle). After searching the Raman spectra of common additives in the KnowItAll Raman spectral library, the three peaks matched the spectrum of CaCO_3 . So, Gown #2 material probably contained calcium carbonate. Gown #1 had a dark blue color, and Wrap had a light blue color. The Raman spectra of both materials had three prominent peaks at 688 , 755 , and 1530 cm^{-1} , which could not be assigned to polypropylene. Spectral library search with KnowItAll found a blue pigment, cobalt phthalocyanine, with characteristic peaks at 678 , 744 , and 1529 cm^{-1} . In addition, some other blue pigments, e.g., irgazin blue and direct blue 86, also have a prominent Raman peak around 1530 cm^{-1} . Although the identification was preliminary, the results might indicate that the extra peaks, especially the one at 1530 cm^{-1} , could come from the pigment in the materials. The same dye was probably used in both Gown #1 and Wrap. Gown #1 had a much darker color than Wrap, indicating more pigment was used in Gown #1. The Raman signals of PP from Gown #1 samples were weaker than the other two materials. The presence of a large amount of pigment might affect the Raman analysis. Raman spectrometry might be a suitable tool to detect inorganic additives and pigments, which only had weak IR activities.

Although different PPE materials may have different chemical compositions and additives, only limited types of PPE are used in a hospital or clinic during a specific period. The collected PPE waste would have much simpler and more stable chemical compositions than recycled plastics from municipal recycling programs. The PPE waste would be easy

to sort and allow recyclers to produce high-quality products with more controllable and uniform properties, which could improve the economic feasibility of PPE recycling.

Effects of the treatments on polymer molecular weight

Molecular weight is a critical parameter for polymers, which substantially influences the thermal and mechanical properties of the materials. Therefore, the changes in molecular weight and its distribution need to be closely monitored. The average molecular weights (M_w), polydispersities (PD) and bulk $\text{CH}_3/1000\text{TC}$ of the three types of PPE materials before and after the treatments were investigated in this work (Table 1).

Among the three types of original materials, Wrap had a slightly higher M_w , while the other two gown materials had similar ones. The disinfection treatments did cause somewhat polymer degradation as suspected. The M_w of the materials decreased about 2–7% after the treatments, but no statistically significant changes were observed. For the two gown samples, the autoclave reduced the M_w more, while the two chemical treatments degraded the wrap sample more severely. The PDs tended to decrease after the treatments, but slightly higher PDs were found on the autoclave treated gown samples. Again, no statistically significant differences in PD were observed. The bulk $\text{CH}_3/1000\text{TC}$ value indicates how many CH_3 groups per 1000 total carbon atoms in polymer. Theoretically, it is 333 for polypropylene. The values were close to 333 before and after the treatments for all the samples, confirming that the materials were polypropylene, and the treatments did not notably change their chemical compositions as demonstrated by the IR analysis. In summary, the treatments could somewhat lower the M_w and tend to reduce the PD of the materials. Different treatments had different effects on the three types of materials, but no statistically significant changes were observed. The treated materials were suitable for recycling. However, since the treatments might slightly degrade the polymers, quicker performance loss of the recycled materials might be observed if the materials were repeatedly used to make medical PPE and recycle.

TGA analysis

Thermogravimetric analysis (TGA) is an important tool to evaluate thermal stability of polymers, which could affect the processing conditions of recycled PPE materials and the performance of resulted products. The TGA results of the PPE before and after the treatments are presented in Fig. 3 and Table 2.

Among the three types of original materials, the thermal stability slightly increased in the order of Gown #2, Wrap,

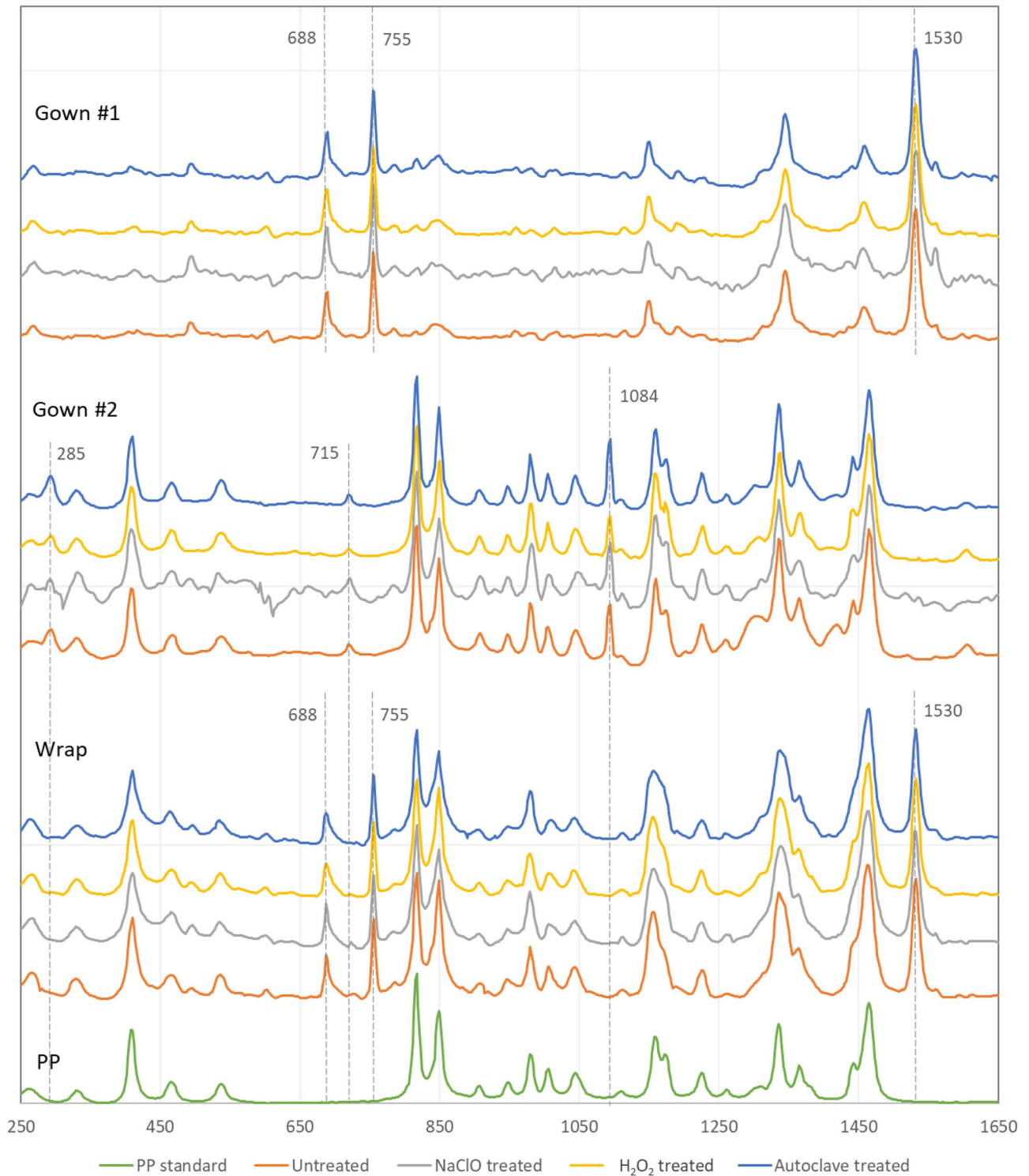


Fig. 2 Raman spectra of the three types of PPE materials with or without treatments

and Gown #1. The treatments affected the three types of materials differently. For Gown #2 and Wrap, thermal degradations of the treated samples took place at significantly higher temperatures with significantly greater maximum

rates. The treated samples had better and more uniform thermal stabilities. The disinfection treatments decreased the M_w but increased the thermal stabilities of the two types of materials. It might be because that the treatments removed some

Table 1 Effects of different treatments on average molecular weights (M_w), polydispersities (PD) and bulk $CH_3/1000TC$

| Type | Treatment | M_w (10^3 g/mol) | M_w Change | PD (M_w/M_n) | Bulk $CH_3/1000TC$ |
|---------|-------------------------------|-----------------------|--------------|------------------|--------------------|
| Gown #1 | N/A | 123 ± 1^a | - | 4.5 ± 0.1^a | 332 ± 1^a |
| | NaClO | 118 ± 7^a | -4.1% | 4.0 ± 0.3^a | 322 ± 4^a |
| | H ₂ O ₂ | 120 ± 4^a | -2.4% | 4.1 ± 0.1^a | 331 ± 3^a |
| | Autoclave | 114 ± 7^a | -7.3% | 4.8 ± 1.0^a | 329 ± 2^a |
| Gown #2 | N/A | 128 ± 8^a | - | 6.2 ± 1.2^a | 327 ± 1^a |
| | NaClO | 126 ± 10^a | -1.6% | 4.8 ± 1.0^a | 330 ± 6^a |
| | H ₂ O ₂ | 126 ± 9^a | -1.6% | 5.3 ± 0.4^a | 327 ± 4^a |
| | Autoclave | 122 ± 3^a | -4.7% | 6.9 ± 1.0^a | 335 ± 9^a |
| Wrap | N/A | 136 ± 5^a | - | 5.3 ± 1.1^a | 332 ± 4^a |
| | NaClO | 130 ± 3^a | -4.4% | 4.8 ± 1.0^a | 326 ± 3^a |
| | H ₂ O ₂ | 129 ± 4^a | -5.1% | 4.5 ± 0.6^a | 331 ± 5^a |
| | Autoclave | 132 ± 1^a | -2.9% | 4.1 ± 0.1^a | 326 ± 2^a |

The data presented are the average of the results from three independent experiments, and the errors represent standard deviations. The values indicated with the same superscript letter within the same PPE materials are not significantly different at the 0.05 level based on Tukey's HSD test

weak parts of the materials, which were easy to degrade. Polymers with lower M_w often have lower thermal degradation temperatures, but it has also been reported that some polymers could have an elevated degradation temperature with lower M_w in some cases [26]. For Gown #1, the results were mixed. The autoclave also significantly increased the degradation temperature and maximum rate. But the NaClO

and H₂O₂ treatments did not significantly affect the decomposition temperatures and maximum rates.

The residues of Gown #1 and Wrap samples were low. But all Gown #2 samples had about 18% residues, which were substantially higher than pure polypropylene should have. Raman analysis had suggested that Gown #2 material might contain CaCO₃. Twenty grams of Gown #2 sample

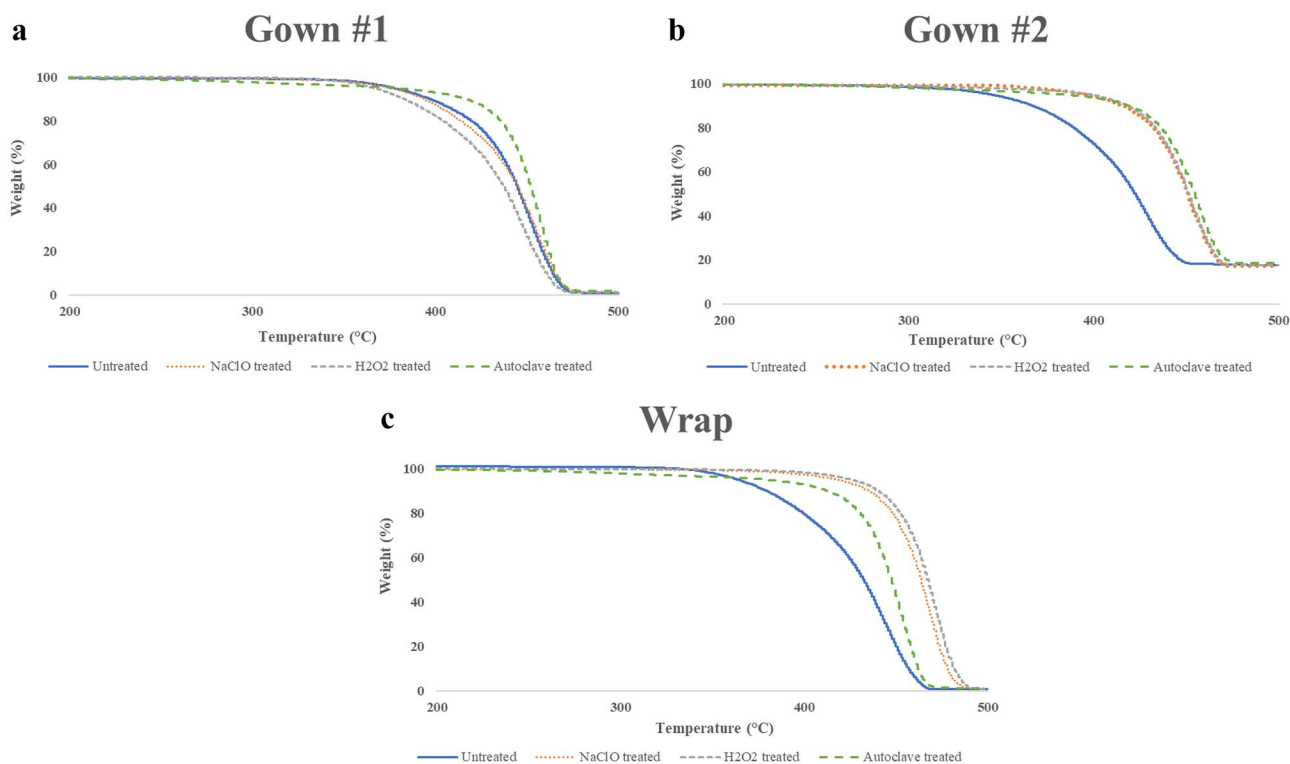
**Fig. 3** TGA curves of PPE materials with different treatments: **a** Gown #1, **b** Gown #2, and **c** Wrap

Table 2 Effects of different treatments on thermal stability

| Type | Treatment | Onset Temperature (°C) | DTG maximum rate (%/°C) | Mass residue (%) |
|---------|-------------------------------|--------------------------|-------------------------|-------------------------|
| Gown #1 | N/A | 422.8 ± 0.6 ^a | 2.3 ± 0.1 ^a | 1.1 ± 0.2 ^a |
| | NaClO | 421.6 ± 3.9 ^a | 2.4 ± 0.2 ^a | 0.7 ± 0.7 ^a |
| | H ₂ O ₂ | 417.7 ± 2.0 ^a | 2.4 ± 0.2 ^a | 1.1 ± 0.3 ^a |
| Gown #2 | Autoclave | 436.4 ± 0.6 ^b | 3.2 ± 0.1 ^b | 1.2 ± 0.6 ^a |
| | N/A | 392.7 ± 2.0 ^a | 1.5 ± 0.1 ^a | 17.5 ± 0.1 ^a |
| | NaClO | 428.5 ± 0.6 ^b | 2.3 ± 0.1 ^b | 17.8 ± 0.3 ^a |
| | H ₂ O ₂ | 431.2 ± 0.6 ^b | 2.4 ± 0.1 ^b | 18.2 ± 0.5 ^a |
| Wrap | Autoclave | 432.0 ± 0.8 ^b | 2.4 ± 0.1 ^b | 18.1 ± 0.5 ^a |
| | N/A | 403.3 ± 1.3 ^a | 1.7 ± 0.1 ^a | 2.4 ± 2.6 ^a |
| | NaClO | 432.6 ± 1.7 ^b | 3.0 ± 0.1 ^b | 2.4 ± 2.6 ^a |
| | H ₂ O ₂ | 434.2 ± 0.3 ^b | 3.2 ± 0.1 ^b | 0.3 ± 0.1 ^a |
| | Autoclave | 428.6 ± 2.1 ^b | 3.1 ± 0.2 ^b | 0.7 ± 0.3 ^a |

The data presented are the average of the results from three independent experiments, and the errors represent standard deviations. The values indicated with the same superscript letter within the same PPE materials are not significantly different at the 0.05 level based on Tukey's HSD test

were heated at 600 °C in a Muffle furnace for 30 min, and a white powder residue was obtained for identification. The Raman spectrum of the residue was acquired, which showed three peaks at 284, 713, and 1088 cm⁻¹. The residue was confirmed to be CaCO₃ based on KnowItAll spectral library search.

In summary, the disinfection treatments tended to improve the thermal stabilities of the PPE materials. The treatments evidently increased the decomposition temperatures and maximum rates of all the materials except for Gown #1 after the NaClO and H₂O₂ treatments. Gown #2 had significantly higher residue levels than the other two materials, which was related to its inorganic additive, CaCO₃.

DSC analysis

Changes in thermal properties could affect the processing parameters of recycled PPE materials. The thermal behaviors, including crystallization peak temperature, crystallization enthalpy, melting peak temperature, melting enthalpy, and crystallinity, of the PPE before and after the treatments were presented in Figs. 4 & 5 and Table 3.

Comparing the three types of original materials, Gown #2 had notably lower crystallization temperature and slightly lower melting temperature. The lower crystallization temperature suggested that the additive in Gown #2 might inhibit the starting of crystallization of the material. Since the CaCO₃ in Gown #2 did not absorb or release heat, Gown #2 showed less enthalpy changes during the melting and crystallization processes. When excluding the mass of CaCO₃, the enthalpy change of Gown #2 was comparable to Gown #1 and Wrap, and the crystallinities of the three types of materials were similar.

The melting and crystallization temperatures of all the materials only slightly varied (about 1–2 °C) after all the treatments, suggesting the treatments would not significantly affect the thermal behaviors of the materials. Therefore, the treated materials could be processed under common PP processing conditions. The crystallinities were around 50% for all the samples before and after the treatments.

All the untreated and treated samples had melting temperatures of about 165 °C, which is the typical melting temperature of isotactic polypropylene. The results confirmed again that the PPE were made of PP fibers and the treatments didn't notably change the chemical composition.

Crystallization kinetics

As an important kinetic parameter in non-isothermal crystallization process, the relative degree of crystallinity (X_t) has been defined as the ratio of the crystallinity at given time to that at infinite time, which can be described with the following equation:

$$X_t = \frac{\int_{T_0}^T \left(\frac{dH_c}{dT} \right) dT}{\int_{T_0}^{T_\infty} \left(\frac{dH_c}{dT} \right) dT}$$

where T_0 and T_∞ are the initial and final temperatures of crystallization, respectively. dH_c is the enthalpy of crystallization released during an infinitesimal temperature interval. T represents the temperature at the crystallization time t .

The evolutions of X_t of the three types of materials before and after the treatments are presented in Fig. 6. All curves were sigma-shaped, indicating that the crystallization accelerated when nuclei gradually formed at the beginning of the process and slowed down when the process was close to the finish.

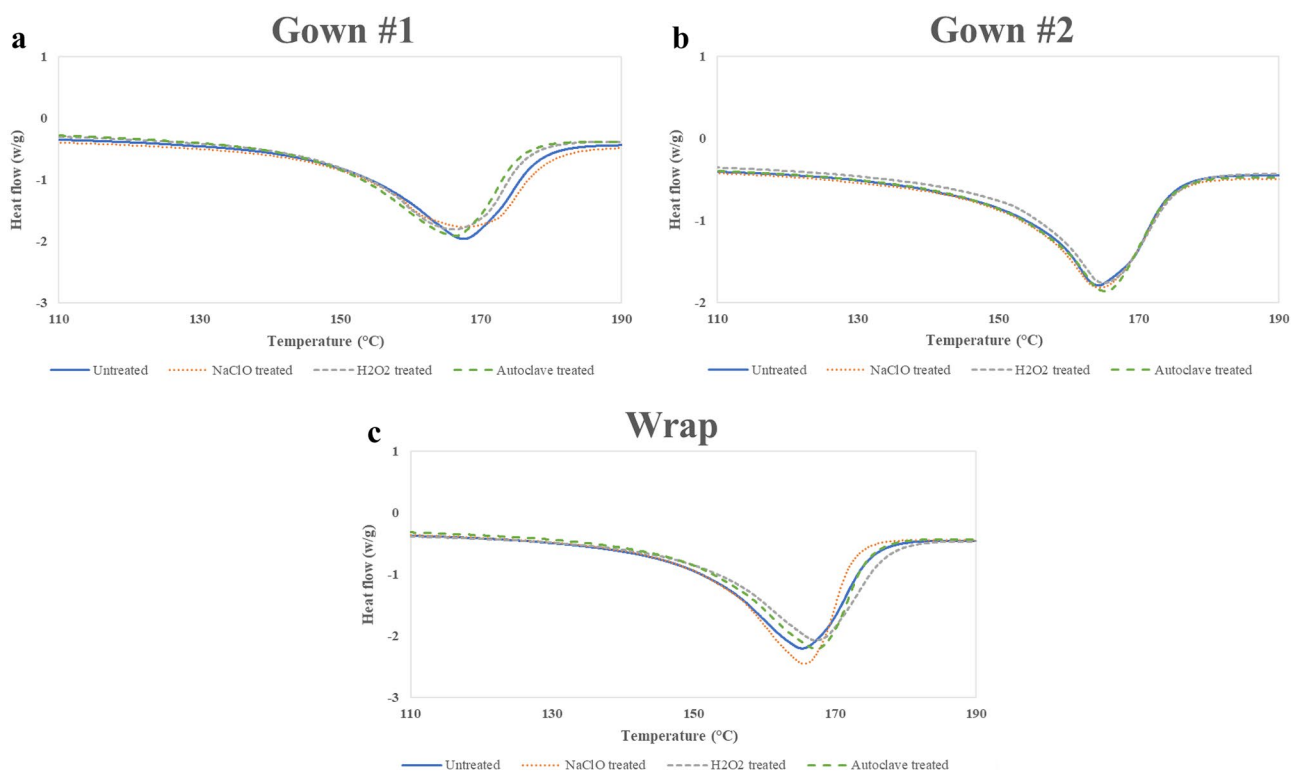


Fig. 4 DSC second heating curves of PPE materials with different treatments: **a** Gown #1, **b** Gown #2, and **c** Wrap

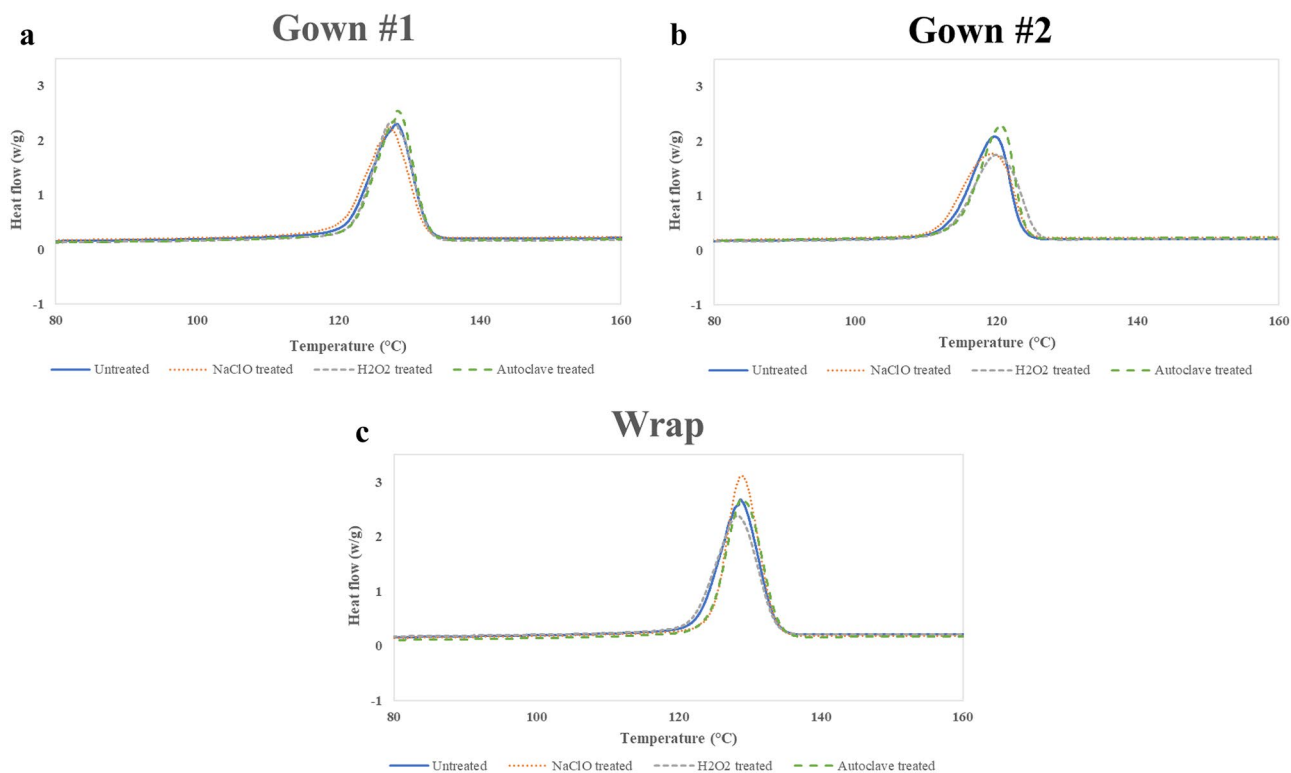


Fig. 5 DSC cooling curves of PPE materials with different treatments: **a** Gown #1, **b** Gown #2, and **c** Wrap

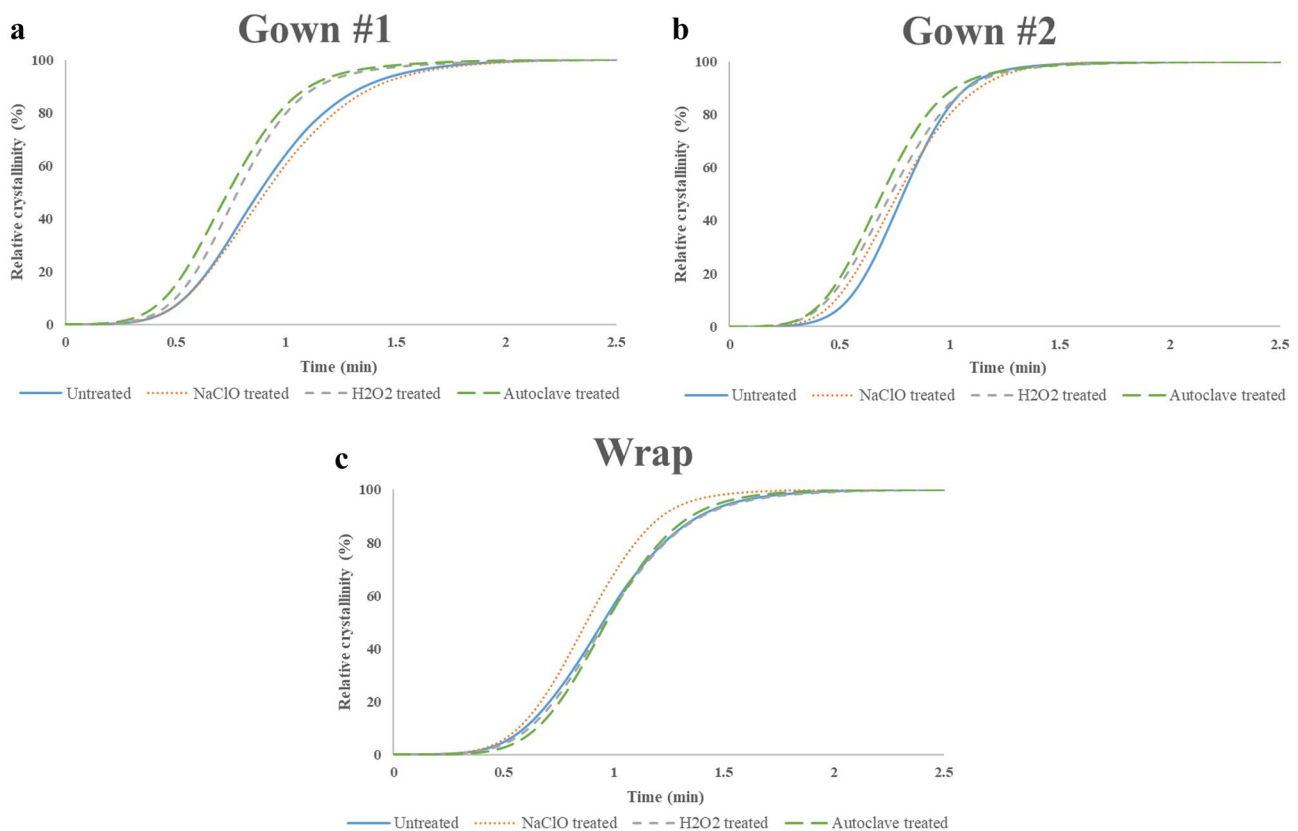
Table 3 Effect of different treatments on thermal behaviors

| Type | Treatment | Crystallization | | Melting | | Crystallinity (%) |
|---------|-------------------------------|--------------------------|--------------------------|--------------------------|--------------------------|-------------------------|
| | | Peak Temperature (°C) | Enthalpy (J/g) | Peak Temperature (°C) | Enthalpy (J/g) | |
| Gown #1 | N/A | 130.1 ± 0.2 ^a | 102.6 ± 0.7 ^a | 165.1 ± 0.2 ^a | 102.4 ± 0.6 ^a | 50.1 ± 0.3 ^a |
| | NaClO | 128.5 ± 0.1 ^a | 112.6 ± 7.5 ^a | 164.9 ± 1.0 ^a | 102.3 ± 1.8 ^a | 49.8 ± 0.9 ^a |
| | H ₂ O ₂ | 130.6 ± 1.0 ^a | 101.1 ± 0.7 ^a | 165.1 ± 0.3 ^a | 100.3 ± 0.9 ^a | 48.9 ± 0.4 ^a |
| | Autoclave | 130.9 ± 0.1 ^a | 101.8 ± 0.4 ^a | 164.5 ± 0.1 ^a | 103.5 ± 0.3 ^a | 50.6 ± 0.1 ^a |
| Gown #2 | N/A | 123.6 ± 1.8 ^a | 88.2 ± 1.9 ^a | 163.2 ± 0.5 ^a | 89.4 ± 2.3 ^a | 52.4 ± 1.1 ^a |
| | NaClO | 122.4 ± 1.4 ^a | 82.1 ± 2.4 ^a | 163.7 ± 0.8 ^a | 81.2 ± 2.3 ^a | 47.7 ± 1.1 ^a |
| | H ₂ O ₂ | 125.3 ± 1.4 ^a | 82.9 ± 2.4 ^a | 163.8 ± 0.8 ^a | 85.3 ± 2.3 ^a | 50.3 ± 1.1 ^a |
| | Autoclave | 124.0 ± 0.3 ^a | 81.5 ± 0.1 ^a | 163.7 ± 0.1 ^a | 83.9 ± 1.3 ^a | 49.1 ± 0.8 ^a |
| Wrap | N/A | 130.0 ± 0.7 ^a | 111.2 ± 0.4 ^a | 165.3 ± 0.2 ^a | 108.9 ± 2.9 ^a | 53.9 ± 1.4 ^a |
| | NaClO | 130.0 ± 0.5 ^a | 107.2 ± 2.6 ^a | 165.3 ± 1.4 ^a | 110.6 ± 2.1 ^a | 54.8 ± 1.0 ^a |
| | H ₂ O ₂ | 130.6 ± 0.1 ^a | 105.2 ± 0.1 ^a | 164.7 ± 0.1 ^a | 103.9 ± 1.2 ^a | 50.5 ± 0.6 ^a |
| | Autoclave | 130.4 ± 0.3 ^a | 106.5 ± 0.6 ^a | 165.2 ± 0.1 ^a | 107.4 ± 1.5 ^a | 52.2 ± 0.7 ^a |

The data presented are the average of the results from three independent experiments, and the errors represent standard deviations. The values indicated with the same superscript letter within the same PPE materials are not significantly different at the 0.05 level based on Tukey's HSD test

All curves ended up with a plateau close to 100%. Although the crystallinities of the samples were not significantly modified, notable effects of the disinfection treatments on the

crystallization processes were observed. In general, a shift of the curve to the left on the time axis suggests a quicker start of the crystallization, while a steeper curve indicates a faster process.

**Fig. 6** The relationships of relative crystallinity and crystallization time before and after the treatments

Crystallization kinetic analysis was carried out with the widely used Avrami equation shown below to obtain more insights of the crystallization processes of the samples [27]:

$$1 - X_t = \exp(-Z_t t^n)$$

With the assumption of constant crystallization temperature, the function could be converted to the double-natural logarithmic form:

$$\ln[-\ln(1 - X_t)] = \ln Z_t + n \ln t$$

where Z_t is the crystallization rate constant and n is the Avrami exponent which depends on the nucleation mechanism and crystal growth dimension. By plotting $\ln[-\ln(1 - X_t)]$ versus $\ln t$, the data can be fitted with a straight line, from which Z_t and n can be obtained from the y-intercept and slope, respectively. Considering the effect of cooling rate, Jeziorny defined a new crystallization parameter Z_c to describe practical non-isothermal crystallization at different cooling rates (Φ) as shown below:

$$\ln Z_c = \frac{\ln Z_t}{\Phi}$$

As shown in Fig. 7, the crystallization process exhibited two stages for all the samples. The second stage had

an evidently lower slope than the first stage. Therefore, the curves were divided into two sections and fitted by the Avrami equation separately. The regression results are listed in Table 4. For all the samples, good linear relationships ($R^2 \geq 0.97$) were observed, suggesting the Avrami model described the crystallization processes well. The Avrami exponent, n , decreased significantly in the second stage for all the samples, which agreed with the slope decrease in the second stage. The n value depends on the crystallization mechanisms and crystal growth dimension [28, 29]. For values of $1 < n < 2$, the growth happens in one dimension with fiber geometry; for $2 < n < 3$, the growth occurs in two dimensions with lamella geometry; for $3 < n < 4$, the growth takes place in three dimensions with spherulites geometry; for $n > 4$, the growth takes place in three dimensions and forms complex spherulite, sheaf-like, or other complicated geometries [30, 31]. The n values ranged between 3.38 and 4.97 in the first stage, suggesting the nuclei had enough space around them and grew in three dimensions, even forming some complicated geometries. However, the n values dropped below 3 and even below 2 for some samples in the second stage. The results indicated that the spherulites might impinge on one another, and there was not enough free space around them. They had to grow in two or even one dimensions. The treatments tended to reduce the n values in most

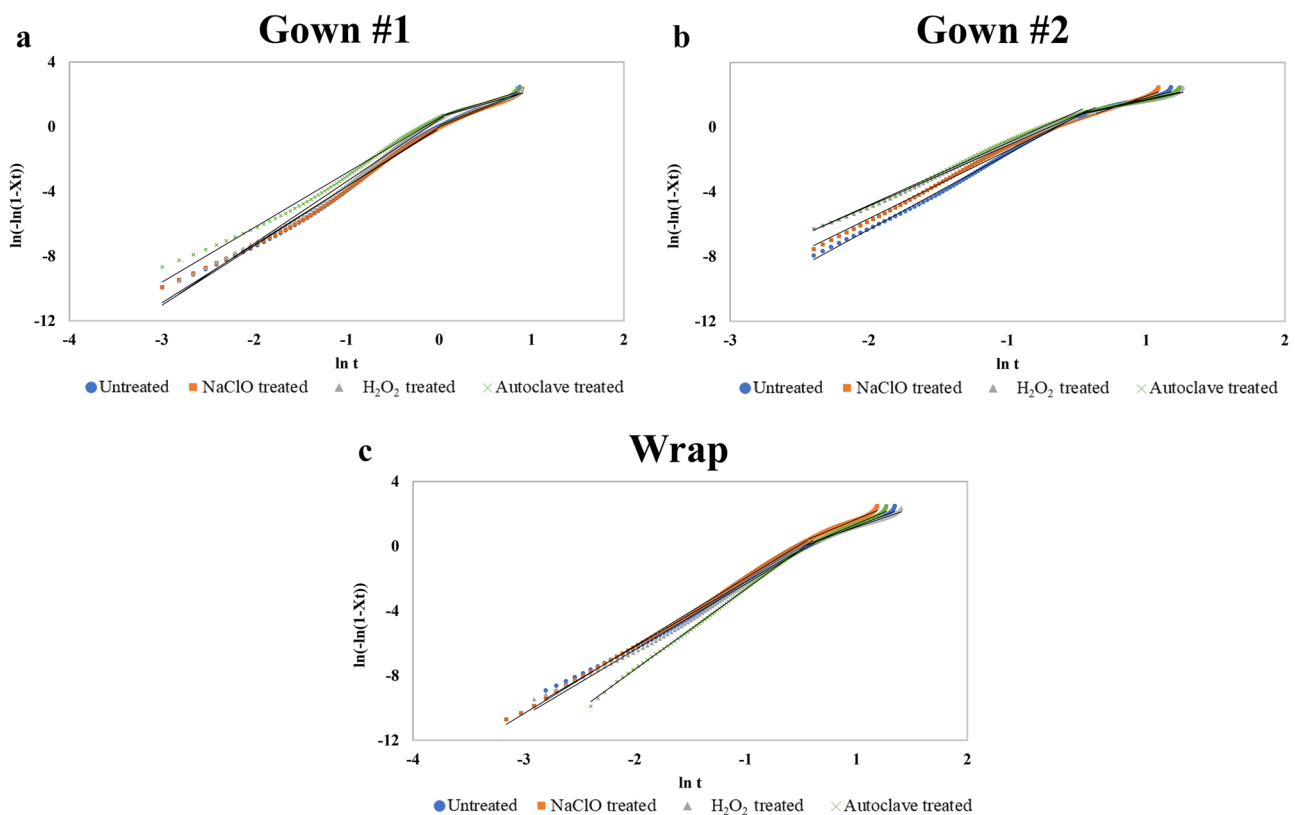


Fig. 7 Plots of $\ln(-\ln(1 - X_t))$ versus $\ln t$ for PPE with different treatments: **a** Gown #1, **b** Gown #2, and **c** Wrap

Table 4 Effects of different treatments on crystallization kinetics

| Type | Treatment | Kinetic Parameters | | | | | |
|---------|-------------------------------|--------------------|------------|-------|------------------|------------|-------|
| | | The first stage | | | The second stage | | |
| | | Z_c (min-n/K) | Exponent n | R^2 | Z_c (min-n/K) | Exponent n | R^2 |
| Gown #1 | N/A | 0.10 | 3.67 | 0.99 | 0.11 | 2.31 | 0.98 |
| | NaClO | 0.09 | 3.59 | 0.99 | 0.10 | 2.33 | 0.99 |
| | H ₂ O ₂ | 0.16 | 3.83 | 0.99 | 0.18 | 1.64 | 0.97 |
| | Autoclave | 0.17 | 3.38 | 0.99 | 0.19 | 1.76 | 0.97 |
| | NaClO | 0.19 | 4.20 | 0.99 | 0.15 | 2.99 | 0.98 |
| | H ₂ O ₂ | 0.21 | 3.74 | 1.00 | 0.21 | 1.85 | 0.97 |
| Wrap | Autoclave | 0.26 | 3.86 | 1.00 | 0.22 | 1.84 | 0.97 |
| | N/A | 0.08 | 4.01 | 1.00 | 0.09 | 2.65 | 0.99 |
| | NaClO | 0.11 | 4.19 | 1.00 | 0.13 | 2.85 | 0.99 |
| | H ₂ O ₂ | 0.07 | 4.08 | 1.00 | 0.10 | 2.33 | 0.99 |
| | Autoclave | 0.08 | 4.97 | 1.00 | 0.09 | 2.90 | 0.99 |

cases, but the NaClO and autoclave treatment increased the n values for Wrap.

The Z_c value indicates the crystallization rate [32, 33]. For all the samples, no essential change in Z_c between the two stages was observed. The results implied that the crystallization rate was less affected, although the crystal geometry was changed in the second stage. Gown #2 samples had evidently higher Z_c values than Gown #1 and Wrap, suggesting higher crystallization rates. Interestingly, the large amount of CaCO₃ in Gown #2 seemed to inhibit the starting of crystallization but accelerated the process once it started. The CaCO₃ might act as a heterogeneous nucleating agent and promote the nucleation rate during the crystallization process. The H₂O₂ and autoclave treatments accelerated the crystallization of Gown #1, the autoclave treatment promoted the process for Gown #2, and the NaClO treatment increased the crystallization rate of Wrap.

Activation energy of crystallization

Since some treatments influenced the crystallization process, the activation energy (ΔE) of crystallization, which is the energy required for the phase transformation to happen, was investigated to understand the process better. In this work, the Kissinger model was employed to calculate the ΔE [34], which was described as following:

$$d \left[\ln \left(\frac{\Phi}{T_p^2} \right) \right] = -\frac{\Delta E}{R} d \left(\frac{1}{T_p} \right)$$

where R is the ideal gas constant and equals 8.314 J/kmol, T_p is the peak crystallization temperature (in K). By plotting $\ln(\Phi/T_p^2)$ versus $1/T_p$, the data can be fitted by a straight line, from which ΔE can be calculated by multiplying the slope by the negative value of R .

The regression results are presented in Table 5. All the R^2 of the samples were greater than 0.98, demonstrating that the Kissinger equation could accurately describe the crystallization process. Negative activation energies were obtained because the crystallization rate increases when the temperature decreases [27, 31]. For the untreated samples, Gown #2 had much lower activation energy than Gown #1 and Wrap, which was consistent with the higher crystallization rate (larger Z_c) of Gown #2. This phenomenon might be caused by the CaCO₃ in Gown #2. Other researchers also found that composites could have lower activation energy and higher crystallization rate when additives were mixed with pure polymers [33, 35]. The NaClO treatment notably increased the activation energies for the Gown #1 and Warp samples, but the corresponding Z_c values only decreased slightly. The H₂O₂ and autoclave treatments didn't significantly change the activation energy for Gown #1, but the related samples showed elevated crystallization rates. The effects of the treatments on the relationship between the activation energy and crystallization rate were still unclear.

Mechanical tension analysis

Tension properties of the untreated and treated PPE are listed in Table 6. The raw Gown #2 had evidently lower maximum force at break than the other two raw materials. The reason probably was that Gown #2 was much thinner than the other two. The treatments tended to slightly increase the maximum forces, especially for Gown #1. However, no statistically significant differences were found after all the treatments for all the materials, suggesting the treatments didn't essentially affect the tension of the materials. The larger differences in tension came from the differences of the raw materials.

Table 5 Effect of different treatments on activation energy of crystallization

| Type | Treatment | Activation Energy | |
|---------|-------------------------------|---------------------|-------|
| | | ΔE (kJ/mol) | R^2 |
| Gown 1# | N/A | -304 | 1.00 |
| | NaClO | -213 | 0.99 |
| | H ₂ O ₂ | -305 | 1.00 |
| | Autoclave | -274 | 0.98 |
| Gown 2# | N/A | -411 | 0.99 |
| | NaClO | -270 | 0.98 |
| | H ₂ O ₂ | -441 | 0.99 |
| | Autoclave | -535 | 0.98 |
| Wrap | N/A | -327 | 0.99 |
| | NaClO | -317 | 1.00 |
| | H ₂ O ₂ | -294 | 1.00 |
| | Autoclave | -298 | 1.00 |

Table 6 Effect of different treatments on tension properties

| Type | Treatment | Maximum Force at Break (N) |
|---------|-------------------------------|----------------------------|
| Gown #1 | N/A | 6.3 ± 0.7 ^a |
| | NaClO | 7.6 ± 0.8 ^a |
| | H ₂ O ₂ | 7.0 ± 0.5 ^a |
| | Autoclave | 7.2 ± 0.1 ^a |
| | NaClO | 1.7 ± 0.1 ^a |
| | H ₂ O ₂ | 1.6 ± 0.1 ^a |
| | Autoclave | 1.6 ± 0.3 ^a |
| | Wrap | N/A |
| Wrap | NaClO | 5.4 ± 0.6 ^a |
| | H ₂ O ₂ | 5.2 ± 0.4 ^a |
| | Autoclave | 5.4 ± 1.0 ^a |

The data presented are the average of the results from three independent experiments, and the errors represent standard deviations. Maximum Force (N) or Ultimate Elongation (%) values indicated with the same superscript letter within the same PPE materials are not significantly different at the 0.05 level based on Tukey's HSD test

Conclusions

The effects of three sterilization treatments (NaClO, H₂O₂, and autoclave) on three types of PPE (Gown #1, Gown #2, and Wrap) were investigated to provide fundamental data for recycling. All three types of PPE were made of isotactic polypropylene fibers, and all the disinfection treatments didn't notably change the chemical composition of the materials. However, all the treatments slightly decreased the M_w and tended to reduce the PD of the polymers, although no statistically significant changes were observed. The treatments had little effect on the thermal properties, crystallinities, and tension properties, while they tended to improve the thermal stabilities and influence the crystallization processes of the materials. Since no detected changes would

significantly affect polymer processing, the treated materials were suitable feedstock for recycling. Meanwhile, evident differences in the raw materials were observed. The three types of PPE materials had notably different initial properties and often behaved differently during the treatments. Gown #2 contained about 18% calcium carbonate, which might result in a higher crystallization rate and a lower crystallization activation energy. But lower crystallization temperature was also observed for Gown #2. Recyclers may need to carefully test the raw materials before processing.

Supplementary Information The online version contains supplementary material available at <https://doi.org/10.1007/s10965-022-03217-w>.

Acknowledgements This work was performed under the financial assistance award 70NANB20H147 from the National Institute of Standards and Technology, U.S. Department of Commerce. The authors would also like to thank the University of Alabama at Birmingham Hospital for providing the PPE for this research.

Declarations

Conflicts of interests The authors declare no conflict of interest.

References

- Overcash M (2012) A comparison of reusable and disposable perioperative textiles: sustainability state-of-the-art 2012. *Anesth Analg* 114:1055–1066. <https://doi.org/10.1213/ANE.0b013e31824d9cc3>
- Conrardy J, Hillanbrand M, Myers S, Nussbaum GF (2010) Reducing medical waste. *Aorn J* 91:711–721. <https://doi.org/10.1016/j.aorn.2009.12.029>
- Ortega R, Gonzalez M, Nozari A, Canelli R (2020) Personal protective equipment and Covid-19. *N Engl J Med* 382:e105. <https://doi.org/10.1056/NEJMc2014809>
- Montgomery M, Hayter A, Klu J, Pieper U (2022) Global analysis of healthcare waste in the context of COVID-19: status, impacts and recommendations (978 92 4 003961 2)

5. Czigiány T, Ronkay F (2020) The coronavirus and plastics. *eXPRESS polymer letters* 14:510–511. <https://doi.org/10.3144/expresspolymlett.2020.41>
6. Nowakowski P, Kuśnierz S, Sosna P, Mauer J, Maj D (2020) Disposal of personal protective equipment during the COVID-19 pandemic is a challenge for waste collection companies and society: a case study in Poland. *Resources* 9:116. <https://doi.org/10.3390/resources9100116>
7. Shareefdeen ZM (2012) Medical waste management and control. *J Environ Prot (Irvine, Calif)* 3:1625–1628. <https://doi.org/10.4236/jep.2012.312179>
8. Grinshpun SA, Yermakov M, Khodoun M (2020) Autoclave sterilization and ethanol treatment of re-used surgical masks and N95 respirators during COVID-19: impact on their performance and integrity. *J Hosp Infect* 105:608–614. <https://doi.org/10.1016/j.jhin.2020.06.030>
9. Card KJ, Crozier D, Dhawan A, Dinh MN, Dolson E, Farrokhanian N, Gopalakrishnan V, Hitomi M, Ho E, Jagdish T, King ES, Krishnan N, Kuzmin G, Maltas J, Mo J, Pelesko J, Scarborough JA, Scott JG, Sedor G, Tian E, Weaver DT (2020) UV Sterilization of Personal Protective Equipment with Idle Laboratory Biosafety Cabinets During the COVID-19 Pandemic. *PLoS One* 16:e0241734. <https://doi.org/10.1371/journal.pone.0241734>
10. Lindsley WG, Martin SB Jr, Thewlis RE, Sarkisian K, Nwoko JO, Mead KR, Noti JD (2015) Effects of ultraviolet germicidal irradiation (UVGI) on N95 respirator filtration performance and structural integrity. *J Occup Environ Hyg* 12:509–517. <https://doi.org/10.1080/15459624.2015.1018518>
11. Yılmaz F, Bahtiyari Mİ (2021) Investigation of the Disinfection Effect of Some Environmental Friendly Applications on Cotton Fabrics. *J Natural Fibers*. <https://doi.org/10.1080/15440478.2021.1944444>
12. Veronesi P, Leonelli C, Moscato U, Cappi A, Figurelli O (2005) Non-incineration microwave assisted sterilization of medical waste. *J Microw Power Electromagn Energy* 40:211–218. <https://doi.org/10.1080/08327823.2005.11688546>
13. Gupta M, Bandi SA, Mehta S, Schiraldi DA (2008) Decolorization of colored poly (ethylene terephthalate) bottle flakes using hydrogen peroxide. *J Appl Polym Sci* 107:3212–3220. <https://doi.org/10.1002/app.27468>
14. Baig GA, Carr CM (2014) A Study on Damage to PLA Knitted Fabrics During Scouring and Bleaching. *Pol J Chem Technol* 16:45–50. <https://doi.org/10.2478/pjct-2014-0049>
15. Rowan NJ, Laffey JG (2020) Unlocking the surge in demand for personal and protective equipment (PPE) and improvised face coverings arising from coronavirus disease (COVID-19) pandemic—implications for efficacy, re-use and sustainable waste management. *Sci Total Environ* 752:142259. <https://doi.org/10.1016/j.scitotenv.2020.142259>
16. Grant K, Andruchow JE, Conly J, Lee DD, Mazurik L, Atkinson P, Lang E (2021) Personal protective equipment preservation strategies in the covid-19 era: A narrative review. *Infection Prevention in Practice* 3:100146. <https://doi.org/10.1016/j.infpip.2021.100146>
17. Centers for Disease Control and Prevention (2016) Chemical disinfectants: Guideline for disinfection and sterilization in healthcare facilities 2008
18. Boborodea A, O'Donohue S (2015) Characterization of Polypropylene in Dibutoxymethane by High-Temperature Gel Permeation Chromatography with Triple Detection. *Int J Polym Anal Charact* 20:724–732. <https://doi.org/10.1080/1023666X.2015.1081136>
19. Wielage B, Lampke T, Marx G, Nestler K, Starke D (1999) Thermogravimetric and differential scanning calorimetric analysis of natural fibres and polypropylene. *Thermochim Acta* 337:169–177. [https://doi.org/10.1016/S0040-6031\(99\)00161-6](https://doi.org/10.1016/S0040-6031(99)00161-6)
20. Blaine RL (2010) Determination of polymer crystallinity by DSC. TA123
21. Blaine RL (2002) Thermal applications note. *Polym Heats of Fusion*
22. Kilinc FS (2015) A review of isolation gowns in healthcare: fabric and gown properties. *J Eng Fibers Fabr* 10:180–190. <https://doi.org/10.1177/155892501501000313>
23. Furniss BS (1989) Vogel's textbook of practical organic chemistry. Pearson Education India
24. Andreassen E (1999) Infrared and Raman spectroscopy of polypropylene. In *Polypropylene* (pp. 320–328). Springer
25. Abdel-Hamid H (2005) Effect of electron beam irradiation on polypropylene films—dielectric and FT-IR studies. *Solid-State Electron* 49:1163–1167. <https://doi.org/10.1016/j.sse.2005.03.025>
26. Ye L, Liu M, Huang Y, Zhang Z, Yang J (2015) Effects of Molecular Weight on Thermal Degradation of Poly (α -methyl styrene) in Nitrogen. *J Macromol Sci Part B* 54:1479–1494. <https://doi.org/10.1080/00222348.2015.1094645>
27. Qiao Y, Jalali A, Yang J, Chen Y, Wang S, Jiang Y, Hou J, Jiang J, Li Q, Park CB (2021) Non-isothermal crystallization kinetics of polypropylene/polytetrafluoroethylene fibrillated composites. *J Mater Sci* 56:3562–3575. <https://doi.org/10.1007/s10853-020-05328-5>
28. Wang J, Dou Q (2007) Non-isothermal crystallization kinetics and morphology of isotactic polypropylene (iPP) nucleated with rosin-based nucleating agents. *J Macromol Sci Part B Phys* 46:987–1001. <https://doi.org/10.1080/00222340701457311>
29. Buzarovska A (2004) Crystallization of polymers (2nd edition) Volume 2: Kinetics and mechanisms. Edited by Leo Mandelkern. Cambridge University Press, Cambridge, 2004. ISBN 0 521 81682 3. pp 478. *Polym Int* 54:1466–1467. <https://doi.org/10.1002/pi.1883>
30. Zhang J, Chen S, Jin J, Shi X, Wang X, Xu Z (2010) Non-isothermal melt crystallization kinetics for ethylene–acrylic acid copolymer in diluents via thermally induced phase separation. *J Therm Anal Calorim* 101:243–254. <https://doi.org/10.1007/s10973-009-0619-x>
31. Montanheiro TL, de Menezes BR, Montagna LS, Beatrice CA, Marini J, Lemes AP, Thim GP (2019) Non-Isothermal Crystallization Kinetic of Polyethylene/Carbon Nanotubes Nanocomposites Using an Isoconversional Method. *J Compos Sci* 3:21. <https://doi.org/10.3390/jcs3010021>
32. Chen S, Jin J, Zhang J (2011) Non-isothermal crystallization behaviors of poly (4-methyl-pentene-1). *J Therm Anal Calorim* 103:229–236. <https://doi.org/10.1007/s10973-010-0957-8>
33. Wang S, Zhang J (2014) Non-isothermal crystallization kinetics of high density polyethylene/titanium dioxide composites via melt blending. *J Therm Anal Calorim* 115:63–71. <https://doi.org/10.1007/s10973-013-3241-x>
34. Kissinger HE (1956) Variation of peak temperature with heating rate in differential thermal analysis. *J Res Natl Bur Stand* 57:217–221. <https://doi.org/10.6028/jres.057.026>
35. Kourtidou D, Tarani E, Chrysafi I, Menyhard A, Bikiaris DN, Chrissafis K (2020) Non-isothermal crystallization kinetics of graphite-reinforced crosslinked high-density polyethylene composites. *J Therm Anal Calorim* 142:1849–1861. <https://doi.org/10.1007/s10973-020-10085-3>

Publisher's Note Springer Nature remains neutral with regard to jurisdictional claims in published maps and institutional affiliations.

Springer Nature or its licensor holds exclusive rights to this article under a publishing agreement with the author(s) or other rightsholder(s); author self-archiving of the accepted manuscript version of this article is solely governed by the terms of such publishing agreement and applicable law.